Solvation Stages of HCl and HBr in Crystalline Phases with Methanol and Small Ethers: Acid−Ether Cluster Complexes in Amorphous and Crystal Phases

J. Paul Devlin,*,† Joanna Sadlej,‡ Maxwell Hollman,† and Victoria Buch*,§

Department of Chemistry, University of Warsaw, Pasteura 1, 02-093 Warsaw and National Institute of Public Health, 30/34 Chelmska Str., 00-725 Warsaw, Poland, The Fritz Haber Institute for Molecular Dynamics, Hebrew University, Jerusalem 1904, Israel, and Department of Chemistry, Oklahoma State University, Stillwater, Oklahoma 74078

Received: September 29, 2003; In Final Form: January 8, 2004

Solid state solvation of HCl and HBr (i.e., HX acids) was investigated by FTIR spectroscopy, with methanol (MeOH), dimethyl ether (DME), and tetrahydrofuran (THF) acting as solvents. The study is an extension of previous investigations of acid hydrates. Effort was devoted to finding those composition ratios for which the acid and the solvent readily form mixed crystalline and amorphous solids and to the study of the extent of acid solvation in these solids. The results were interpreted with the help of density functional theory (DFT) calculations for $(HX)_n(solvent)_m$ clusters and for protonated solvent ions. A dramatic difference was observed between methanol and ether solvation. For methanol, crystal and amorphous *ionic* solids form with MeOH:HX ratios of 1:1, 2:1, and 3:1, in analogy to the hydrate case. The parallel to the HX−hydrate series apparently extends to the formation of the methanol analogues of the hydronium and Zundel cations, for the corresponding solvent−acid ratios. In contrast, mixed acid−ether solids tend to be *acid-rich; n*ew crystal solids were discovered, with HX−ether ratios of 6:1, 4:1, 2:1, and 1:1. In the limit of high acid−ether ratio, the acid is clearly molecular. In the 1:1 crystals, very intense and broad bands in the 800−1500 cm^{-1} range suggest proton sharing between the halide and the O atom of the ether; and a Zundel-like species [ether..H^+..X^-] is suggested as the basic unit. Such units polarize, mutually solvate, and stabilize each other. In the case of HCl, the Zundel unit appears to persist to intermediate acid:ether ratios, despite dilution by the extra acid. However, in the case of 2:1 and 4:1 HBr−THF, the acid is fully *molecular*, though perturbed significantly by solvation.

1. Introduction

Solvation in the solid phase is of a basically different nature than for a liquid. A flexible liquid solvent forms readily a solvation shell around an *isolated* solute particle. In contrast, solvation in a crystal is typically a *collective* phenomenon, associated with nucleation of a mixed solid of a well-defined composition and structure. The specific factors determining preferred composition ratios for a given solute−solvent combination are far from being well understood, but generally, they should be determined by the geometry and the bonding properties of the constituents. Reported here are efforts to extend the understanding of solid-state solvation/ionization of hydrohalic acids by computational and spectroscopic study of mixed crystalline phases of HX with methanol and small ether molecules.

Solid-phase *acid* solvation has recently received considerable attention due to the importance of acid hydrates in atmospheric chemistry. Mixed acid-solvent systems display interesting and rich physical chemistry. Four crystal forms are known for HCl hydrates. These hydrates are all ionic and include Cl^- anions and protonated water cations. Well-defined cation forms, either Zundel $(H_5O_2)^+$ or hydronium H_3O^+, can be found, depending on the composition. Based on X-ray determinations of structures, the following formulas were proposed:[1] for the monohydrate, $(H_3O^+)(Cl^-)$; for the dihydrate, $(H_5O_2)^+(Cl^-)$; for the trihydrate, $(H_5O_2)^+(H_2O)(Cl^-)$; and for the hexahydrate, $(H_9O_4)^+(H_2O)_2(Cl^-)$ (the cation in this structure corresponds to an Eigen form, i.e., a hydronium cation fully solvated by three water molecules).

FTIR spectroscopy of crystal and amorphous hydrohalic acid hydrates was pursued by us in the past.[2,3] The spectra of crystal $(HCl)(H_2O)_{n=1-3}$ are shown in Figure 1A. Spectra of the hydronium and Zundel ions (solvated by Cl^-) can be seen most clearly in the spectra of the mono- and dihydrate, respectively. The spectra of the crystal di- and trihydrates and deuterates display an underlying continuum. This "Zundel" effect,[4] which will also be discussed below for other systems, is summarized briefly here. The continuum absorption is characteristic of proton-sharing species, such as $(H_5O_2)^+ = H_2O\cdot\cdot H^+\cdot\cdot OH_2$, in condensed (solid and liquid) phases. The effect is due to continuous modulation of the proton potential; by the O···O stretch, by other local motions, and by fluctuations of the electric field. Thus, the proton potential varies from a single well for short O···O distances, to either symmetric or asymmetric double wells.[4,5] The proton motion modulates in turn the local intermolecular interactions; for example, H^+ approach to one of the bonded molecules affects its stretch and bending force constants. As a result, even crystal phases display broad bands and underlying continua. In the corresponding amorphous phases, the relative contribution of the continuum absorption is

* To whom correspondence should be addressed. (J.P.D.) E-mail: devlin@okstate.edu. (V.B.) E-mail: viki@fh.lhuji.ac.il.
† Oklahoma State University.
‡ University of Warsaw and National Institute of Public Health.
§ Hebrew University.

10.1021/jp036909w CCC: $27.50
Published on Web 02/18/2004

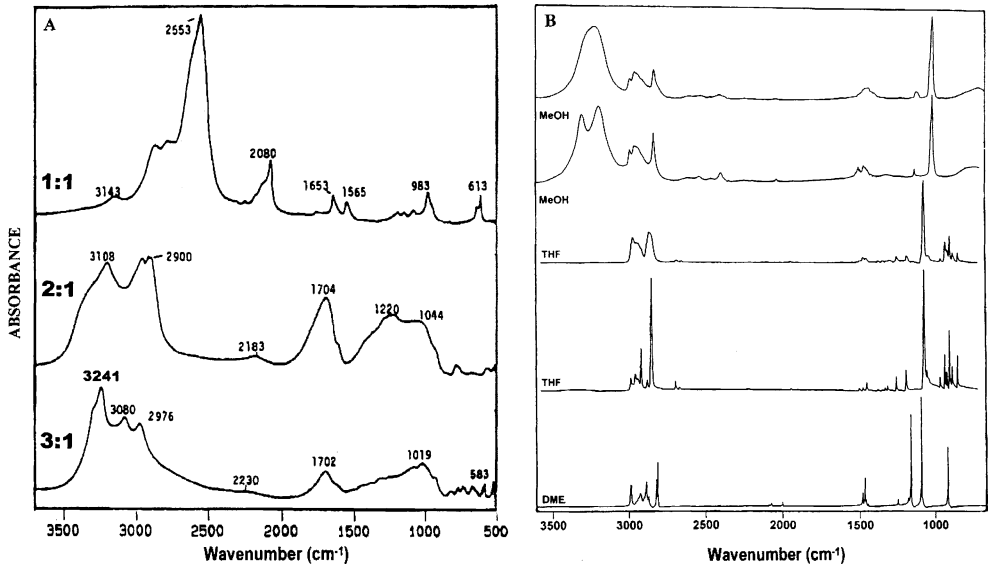

Figure 1. Survey spectra from the top down: (A) of crystalline thin films of the monohydrate, dihydrate and trihydrate of HCl and (B) of thin solid films of amorphous MeOH, crystalline MeOH, amorphous THF, crystalline THF, and crystalline DME.

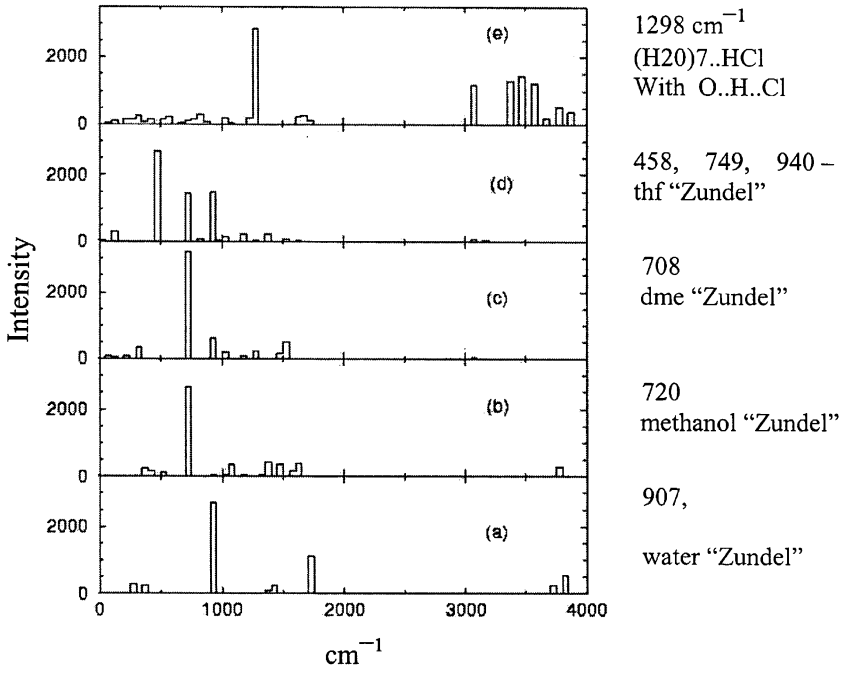

Figure 2. Harmonic DFT spectra of five model systems which include proton-sharing between two heavy atoms. Frequencies of intense bands are listed in the right margin. The respective minimum energy configurations are shown in Figure 3.

enhanced by the presence of a frozen broad distribution of equilibrium configurations.

Figure 2 shows density functional theory (DFT) computed spectra of a number of model molecular species with a proton shared between two heavy atoms, including the Zundel ion $(H_5O_2)^+$. The corresponding model structures are shown in Figure 3. By far the most intense infrared transitions correspond to the localized vibration of the shared proton between the two heavy atoms or to extended excitations with a substantial contribution from this proton motion (the asymmetric stretch). The exact calculated frequencies should not be taken too seriously, since harmonic approximation was used, whereas in proton-sharing systems, very large anharmonic shifts amounting to hundreds of cm^{-1} are possible.[6] Moreover, in condensed phases, one expects strong long-range coupling between vibrations of adjacent protons and between the proton motion and other system vibrations. On the other hand, the basic qualitative signature of proton sharing, obtained in DFT, in the form of very intense transitions in the 800∼1500 cm^{-1} range, is likely to be correct. We thus assign the broad feature at ∼1100 cm^{-1} in the dihydrate spectrum (Figure 1A) to the asymmetric $H_5O_2^+$ proton stretch, broadened by coupling to other motions. Moreover comparison to DFT spectra suggests assignment of the dihydrate feature at 1700 cm^{-1} to water bending "illuminated" by coupling to the proton motion. For a recent example of such broad asymmetric-stretch bands in a proton sharing crystal system, see a study of "proton sponges".[7]

Comparison of the dihydrate to protonated-water spectrum in a liquid acid solution is of interest. There, the cation undergoes continuous interconversion between the Zundel and the hydronium forms, and the spectrum corresponds to a very broad continuum extending from ∼800 to ∼3000 cm^{-1}.[4,5] In the crystal hydrate, the more rigid periodic structure results in a distinct, albeit broad, Zundel asymmetric stretch band.

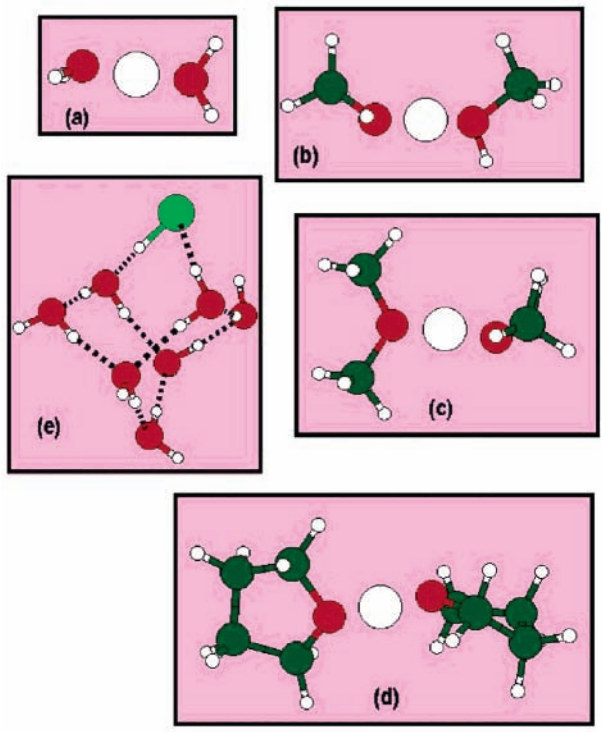

Figure 3. Structures of model systems which include proton sharing by two heavy atoms, used to derive ab initio spectra of Figure 2. Structures (a−d) correspond, respectively, to a Zundel analogue in which the proton (large white circle) is shared by two O atoms of water (a), methanol (b), DME (c), and THF (d). (a−d) DFT-B3LYP calculation in the aug-cc-pvDZ basis set. Structure (e) of $(H_2O)_7HCl$ was adopted from ref 10; this structure examplifies proton sharing between two different heavy atoms, O and Cl; H···Cl = 1.431 Å; H···O = 1.381 Å. (e): MP2 calculation in aug-cc-pvDZ basis.

Presence of the underlying broad continuum suggests, however, occasional large-amplitude structural distortions in the crystal dihydrate as well.

Though molecular clusters of complexes of hydrohalic acids with *small* ethers have been a subject of several spectroscopic[8−10] and computational[11] studies over the past 30 years, there is little structural or spectroscopic information about the corresponding crystal phases. In fact, solid phase data are apparently limited to results of infrared studies of primarily amorphous samples generated by mixing halide acids with dimethyl ether (DME) at low temperatures,[12] though related spectra have also been reported for samples of warmed inert matrixes containing HI-DME complexes.[13] (An extensive study has also been reported for cold *amorphous* mixtures of HX acids with the solvent acetone.[14]) Even less information is available for solid-phase methanol (MeOH) mixed with hydrohalic acids, though the interaction of HBr with cold ethanol films has been the object of a recent reactive-ion-scattering study.[15] The lack of information on these potentially interesting crystal systems reflects their instability at temperatures above 200 K as a result of the high component vapor pressures. Here we describe how both crystalline and amorphous thin films of formulas mMeOH:HX and nHX:ether (where HX is HBr, or HCl, ether is tetrahydrofuran (THF) or dimethyl ether (DME), $m = 1-3$ and $n = 1, 2, 4$, and 6) can be studied using standard low-temperature FTIR absorbance spectroscopy and characterized using insights from DFT computations.

The published data on the acid−ether small clusters are informative for the solid-state systems of interest here. Results from infrared matrix-isolation[8,9] and supersonic jet-FTIR spectroscopy, together with density-functional theory calculations,[10] have been reported for the 1:1 complex of HCl with DME. The theory of Witkowski and Marechal[16] has been applied by Wojcik[11] to the interpretation of band progressions in the H−Cl stretch mode of mixed-dimer spectra obtained by the supersonic-jet approach. The matrix spectra also include data for the 2:1 and 1:2 HX:DME complexes with the results for the H−X stretch modes summarized by Barnes and Wright.[8a] The mixed-dimer frequency for HCl (HBr) is 2310 (2050) cm^{-1}, whereas a single band at 2480 (2240) cm^{-1} was assigned to the 2:1 complex. The 1:2 complex revealed an HX band at 1980 (1740) cm^{-1}. These matrix data correlate well with frequencies calculated using density functional theory (vide infra).

The solvation/ionization of HX can be controlled by varying the solvating groups of a selected series of solvents. The O−H group participates actively in the solvation of HX molecules/ions within the ionic crystalline hydrates,[1,3] the MeOH−HX clusters and solids (vide infra), and at the ice surface[3,17,18] and plays a major role in the dissociation of HX into ions within clusters of H_2O molecules.[19,20] Past studies indicate that HCl dissociation requires a minimum of three hydrogen bonds: one to H and two to Cl.[3,17−19] Thus, the stepwise decrease of the O−H population, through the series H_2O, MeOH, and R_2O (ether molecules, e.g., THF or DME), gives access to variations in acid-solvation stages. In the case of H_2O and MeOH, the ionic form of HX is the stable one for all crystal phases. By contrast, HX−ether solid phases, absent O−H groups, may lack solvation-induced acid dissociation. As a result, the multiple acid-ether *crystalline phases*, described here for the first time, create a unique opportunity to observe a remarkable range of molecular−HX solvation for fixed and (potentially) defined configurations. The range appears to extend from slightly perturbed acid molecules, to full proton-sharing with the ether O-atom.

Stepwise solvation of HX was studied by us in the past in a different system: low-temperature HX adsorbates on ice nanoparticles.[3,17] Surfaces of crystalline ice nanoparticles are characterized by a low density of dangling O and H atoms. Therefore, at low *T*, their surface is a relatively poor solvating medium, so adsorbate one- and two-coordinated *molecular*-acid molecules can be readily observed. The former are slightly stretched, whereas the latter, being strongly stretched, are on the verge of ionization. The corresponding H−X stretch-mode frequencies for adsorbed HCl (HBr), at 2480 (2260) and 1710 (1530) cm^{-1} (as compared to the gas-phase value of 2891 (2560) cm^{-1}), reflect different levels of acid solvation in accord with ab initio calculations for model surface sites.

Shifts of such magnitudes might seem unlikely from solvation by ether molecules which lack the OH groups so important to solvation by water. However, the matrix-isolation[8,9] and condensed-phase[12] data indicate that large shifts of the H−X bands occur in small-ether systems. Further, HX molecules are known to ionize to a degree in liquid ether solvents and when incorporated within polymers of ethylene oxide.[21] Such behavior suggests that solvation of HX by small-ether molecules, within a series of amorphous or crystalline condensed phases, will induce infrared-band frequency shifts of a range comparable to that observed for the HX−ice surface interaction. Indeed, as the solid-state acid−ether ratios are reduced, the evolution of ether-solvated HX, from very slightly distorted to structural analogues of the Zundel cation will be noted. Moreover, the presence of multiple solvation states within individual crystalline forms offers the opportunity for study of preferential positioning

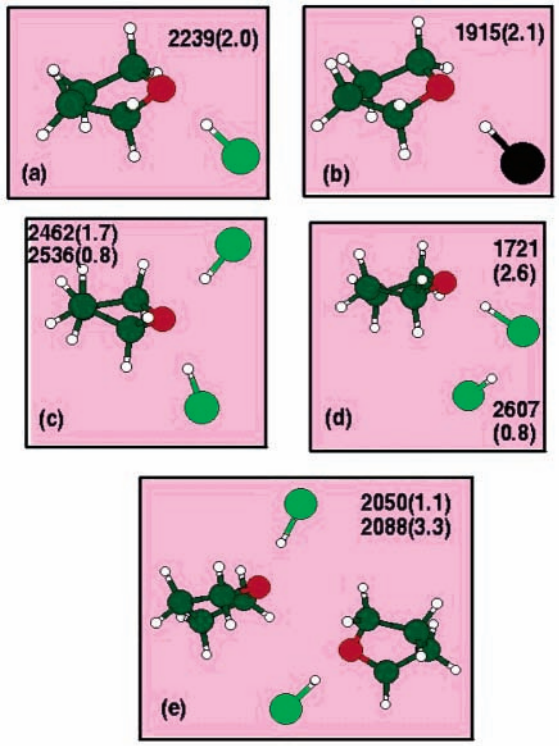

Figure 4. Model structures of acid−THF clusters of different compositions, studied by DFT-B3LYP calculations. C, small, black; H, white; O, red; Cl, green; Br, large, black. In each panel, HX harmonic frequences are marked, in cm^{-1}. The intensity is given in brackets, in thousands of kM/mol. The isolated HCl (HBr) frequency at this level of calculation is 2925 (2597) cm^{-1}.

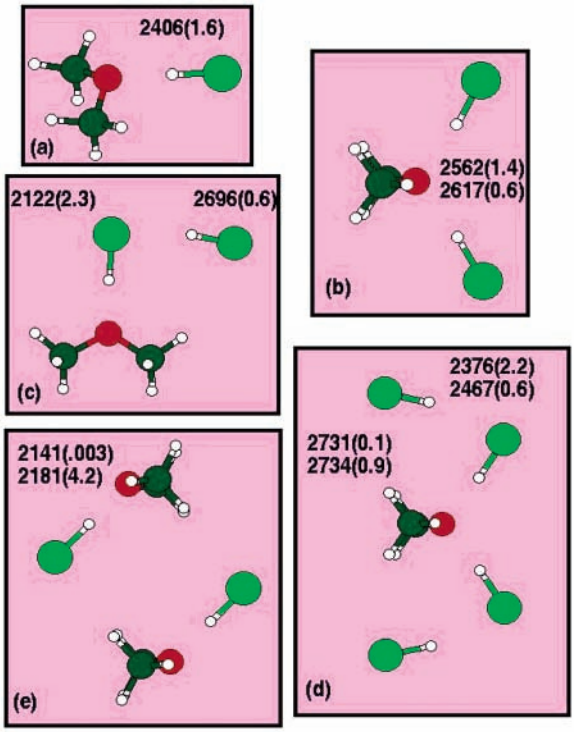

Figure 5. Model structures of acid−DME clusters of different compositions, studied by DFT-B3LYP calculations. C, black; H, white; O, red; Cl, green. In each panel, HX harmonic frequences are marked, in cm^{-1}. The intensity is given in brackets, in thousands of kM/mol.

of chloride vs bromide and/or hydrogen vs deuterium. Data for mixtures of HCl, HBr, DCl, and DBr, within the 2:1-crystal system, will be examined to address this question of preferential occupancy of sites, in addition to aiding in the general interpretation of the spectra of the crystalline phases.

To aid the interpretation of the experimental results, we performed a series of DFT-B3LYP calculations for a number of model cluster systems, containing acid and solvent in different ratios. The models and the acid frequencies are shown in Figures 4 and 5. The DFT calculations for the clusters and also for proton-sharing systems (mentioned above) are summarized in the Appendix. The cluster frequencies are not expected to match those of an extended solid, even if the solid can be viewed in fact as an extended array of the cluster units. This is because of mutual solvation of such units in the condensed phase. Still, considerable insight can be gained from the calculations. Note, for example, an *increase* in HCl frequency upon attachment of a second HCl to the ether O-atom (Figure 4a,c; Figure 5a,b), and the *decrease* upon attachment of additional HCl in tandem, as in O..HCl..HCl (Figure 4a,d; Figure 5a,c). Note also the decrease of the acid frequencies in the cyclic $(HCl)_2(ether)_2$ cluster, with respect to the HCl-ether dimer, due to many-body effects (Figure 4a,e; Figure 5a,e). It will be shown that these effects are much more dramatic for the extended 1:1 HX:ether molecular solids.

The methods of sampling and determination of spectra are discussed in section 2. Spectra for the crystalline and some of the corresponding amorphous phases are presented in section 3, together with tentative interpretations largly based on DFT calculations. The results are summarized in section 4. Details of the electronic structure calculations are given in the Appendix.

2. Experimental Section

Thin films of acid-solvent mixed solids were prepared by vapor co-condensation onto a CsI or Silicon substrate supported on the stem of a low-temperature infrared cell. Deposition was through separate glass tubes with 2 mm orifices with the vapors released ∼4 cm from the substrate surface. The substrate was held at ∼80 K for a 10−12 min deposition during which the sample formed as an amorphous film 0.5−1.0 micron thick. The ratio of HX (HCl, HBr, or HI) to solvent in each deposit was determined from flow rates through calibrated flow meters and checked against deposits from premixtures prepared at moderate pressures within large glass bulbs. Flow-meter calibration plots were obtained by monitoring the emergence of interference fringes for a range of flow rates during deposition of individual vapors. Experiments with HI, though completed shortly after preparation of the HI from NaI reaction with concentrated sulfuric acid, were hampered by dissociation to H_2 and I_2, and were, therefore, limited to mixed solids with methanol. Other reagents were purchased commercially and used after outgassing of the liquids or vacuum distillation of more volatile impurities from the gases: methanol (Baker Analyzed); THF (Fisher Certified); gases DME, HCl, HBr (Matheson Research Purity: >99.8%).

Amorphous samples of the desired HBr−THF ratios, prepared in the above manner, were subsequently warmed for crystallization at temperatures appropriate for a particular ratio: 120 K for 6:1, 140 K for 4:1, 160 K for 2:1, and 180 K for 1:1. Temperatures lower by 10−20 K, to minimize loss of HCl to the vapor phase, were optimum for crystallization of the corresponding HCl−ether samples. Because the amorphous films have a significant HX vapor pressure at the respective crystallization temperatures, crystallization in the closed cell was facilitated for deposits containing 5−20% more acid than required by the integer ratios (to account for the acid vapor lost

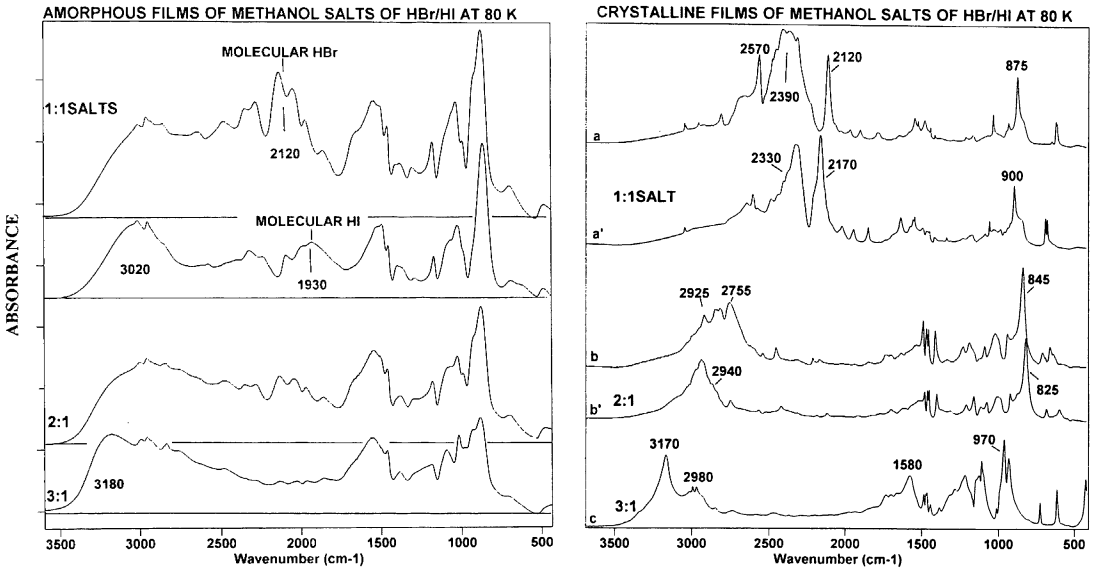

Figure 6. FTIR absorbance spectra of thin amorphous and crystalline films of mMeOH:HX: Left panel, amorphous films of mMeOH: HBr, as labeled (m:1), except for second from top which is of MeOH:HI. Right panel, crystalline films of mMeOH: HX as labeled (m:1). HX is HBr except a′ and b′ for which the acid is HI.

to the cell volume). HCl and HBr each form four crystalline phases with THF, whereas HCl forms five crystalline phases with DME. FTIR absorbance spectra were measured at 80 K for each member of each of these three series. Several of the crystalline phases were also obtained by first crystallizing a 6:1 sample followed by pumping HX from the films at the temperatures noted above to achieve a particular acid-ether phase.

Once a 1:1 crystal was formed, by either approach, crystals of higher acid ratios could also be prepared by exposing that film to an appropriate amount of HX(g) at the proper temperature. In other words, acid molecules move freely in-and-out of the films at temperatures near the respective crystallization temperatures. The rate of gain or loss is related to the diffusion rate of acid molecules through the existing solid. For example, after nucleation of the 2:1 crystal at the 1:1 film surface, the 2:1 crystalline phase is propagated by diffusion of the acid through the 2:1 overlayer to the reaction zone at the interface with the underlying 1:1 crystal. The reverse process, formation of the 1:1 film from the 2:1, requires diffusion of the acid from the interfacial reaction zone to the surface through the 1:1 overlayer (which nucleates at the surface before moving as a front through the film while acid is desorbed to the vapor phase). This behavior suggests that diffusion coefficients can be determined for acids for each of the different crystalline films, as has been reported for ice nanoparticles[22] and microparticles.[23]

Quantitative reaction rates are yet to be determined for the films, but it is remarkable that a complete cycle, from the 4:1 HBr:THF to the 2:1 and back to the 4:1 phase, requires only a few seconds at ∼150 K (when HBr is rapidly removed by pumping to a cryogenic surface and then released to reform the 4:1 film). This ability, to change the crystal phase by using the vapor phase to add or remove HX, greatly facilitates spectroscopic study of variations on the simple crystalline series. For example, data will be presented showing conversion of a 1:1 film of HBr−THF to a crystalline 2:1 film containing equal amounts of HBr and HCl by simple exposure to HCl vapor; and to a 2:1 sample containing equal amounts of H and D by exposure to DCl vapor.

3. Results and Discussion: Spectra of Amorphous and Crystalline Acid−MeOH and Acid−Ether Films

Amorphous and crystalline films have been studied of three different solvent molecules, MeOH, THF, and DME, combined with the hydrohalic acids HCl and HBr (and HI to a limited extent). For convenient reference, the low-temperature survey spectra of the pure solvent thin films are presented in Figure 1B. The MeOH spectrum is dominated by bands of the stretch modes of the O−H, C−H, and C−O bonds near 3300, 3000, and 1000 cm^{-1}, whereas the strong ether bands below 2000 cm^{-1} are produced by C−H bending (near 1450) and a mix of C−O and C−C stretch modes in the 800−1200 cm^{-1} range. In spectra of the solid phases with HX (presented in the next section), other strong solvent features, from combination and overtone states, appear as a result of coupling (both resonant and antiresonant) with the broad HX states.

Ultimate understanding of the crystal structure of the new solids must await an X-ray study. Although one cannot derive the structures from the spectra, considerable insight as to the possible building blocks can be obtained from comparison to DFT calculations (Figures 2−5). For reasons of computational efficiency, HCl rather than HBr was considered in the computational models. The assignments given below should be considered as tentative.

3.1. mMeOH:HX. The FTIR absorbance spectra of amorphous and crystalline films of mMeOH:HBr, with $m = 1-3$, are given in Figure 6. The spectra of the amorphous phases are characterized by intense broad bands with an underlying continuum stretching from ∼800 to near 3000 cm^{-1}. Such continua are common for amorphous phases that contain the Zundel cation ($H_5O_2^+$) (e.g., the amorphous acid hydrates[3]) and can be related to the MeOH analogue $(MeOH)_2H^+$. The individual amorphous phases of Figure 6 (left panel) are distinguished by the blue-shift of bands in the O−H stretch region with increasing m value and by the presence of a pronounced band of partially solvated *molecular* HBr near 2200 cm^{-1} in the $m = 1$ case. (The latter assignment, as the molecular HBr stretch band, follows from comparisons with the amorphous phase of MeOH:HI in Figure 6A, for which the molecular HI-stretch mode occurs at ∼1950 cm^{-1}, and with the monohydrate

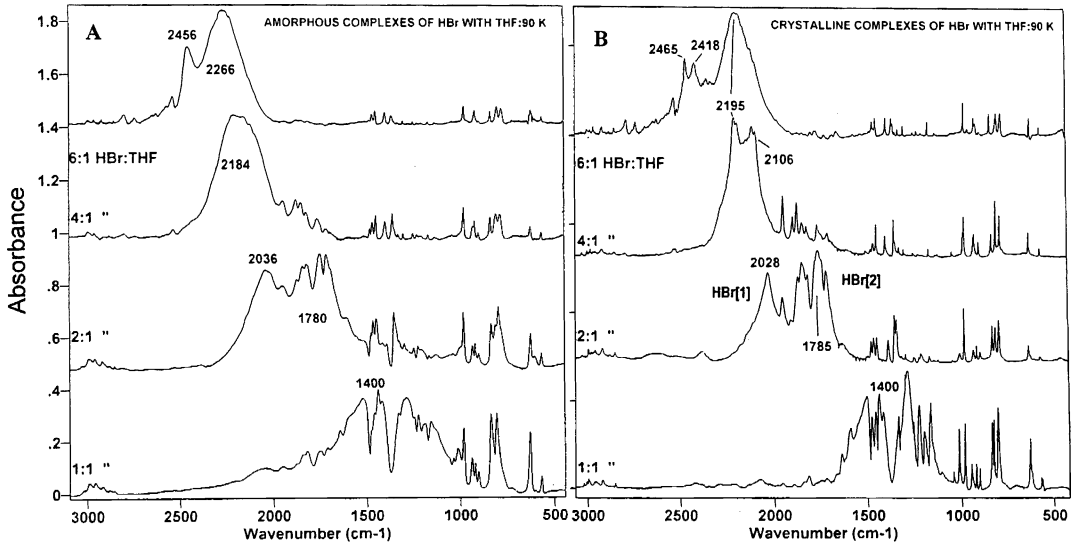

Figure 7. FTIR absorbance spectra of (A) amorphous and (B) crystalline thin films of nHBr:THF identified by the labels *n*/1. Crystalline films, scanned at 80 K, were formed by warming amorphous films prepared at 80 K.

of HCl which has a molecular component within the band near 2550 cm^{-1} [2]).

Strong analogies exist between the spectra (Figure 6B) of the *crystalline* mMeOH:HX members and the corresponding mH_2O:HX hydrate spectra of Figure 1A. In both series, the peak maximum in the "OH" stretch region experiences a stepwise blue-shift with increasing *m* value, from 2500 ± 100 to near 3200 cm^{-1}. A second notable analogy is that the integrated band intensity of the bands between 800 and 1800 cm^{-1}, which in both series for $m = 1$ is much less than that of the O−H stretch modes, increases markedly for $m = 2$ to meet or exceed the intensity in the stretch-mode region. The qualitative similarity between mMeOH:HX and mH_2O:HX spectra suggest a similarity of basic structural units and thus assignment to $(MeOH_2)^+(X^-)$ for $m=1$, $((MeOH)_2H^+)(X^-)$ for $m=2$, and $(MeOH)_2H^+)(MeOH)(X^-)$ for $m = 3$. For $m = 2$ and 3, the high intensity of broad bands in the 800−1800 cm^{-1} range is ascribed to the strong coupling of a series of vibrational excited states to the asymmetric proton stretch of the methanol Zundel cation (see Introduction).

3.2. nHBr:THF. The spectra for this system display a smooth change with composition. It is therefore the first ether system discussed. The amorphous and crystalline FTIR absorbance spectra, for thin films of HBr and THF mixtures with acid−ether ratios of 6, 4, 2 and 1, are presented side-by-side in Figure 7.

Like other spectra of this study, these are characterized by a mixture of relatively narrow solvent bands and unusually broad bands of the HX "molecule"; with the latter bands often fragmented by superposed anti-resonances (or Evan's holes[13,24]) with narrow solvent states. Several strong narrow THF bands result from Fermi resonance between overtone/combination bands of low-lying fundamentals and the intense broad HX transitions.

The spectra of pure THF nanoparticles (Figure 1B), lacking these Fermi-resonance effects, are relatively free of intense bands. When the overtone falls within a broad HX band, the negative Evan's-hole features can be "intense", whereas in the wings of such bands, the overtones often gain unusual positive intensity.[25] This makes it necessary to recognize fragmented HX bands that appear to be multiplets but are actually broad bands with superposed Evan's holes or solvent resonances. The overall effect is one of extremely rich spectra considering the relatively few atoms within the cluster complexes that are thought to make up the crystals.

A comparison of the amorphous and crystalline phase spectra of Figure 7 is particularly revealing. Basically, the difference between the two spectra, *for a given acid−ether ratio*, is one of bandwidth only; that is, when the spectral resolution is degraded to 20 cm^{-1}, it becomes difficult to distinguish an amorphous-phase spectrum from that of the corresponding crystalline phase. The implication of this match between the amorphous and crystalline spectra is a critical one, namely, that both phases must be composed of similar basic structural units.

Given the close parallel between the amorphous and crystalline spectra, it is sufficient to focus on the crystalline-phase spectra of Figure 7B. We consider first the $n = 6$ case. For this and all other ratios, features above ∼2100 cm^{-1}, with the exception of the C−H stretch modes of THF near 3000 cm^{-1}, can be assigned to HBr stretch modes, with the precise band positions indicative of different positions within a basic repeat unit. Other observable features for this 6:1 crystal are weak narrow THF bands between 500 and 1800 cm^{-1}.

Since the broad HBr band is centered near 2200 cm^{-1}, the maximum shift of the H−Br stretch-mode frequency, from the gas-phase value of 2560 cm^{-1},[26] is <500 cm^{-1}. This indicates that the H−Br bond experiences, at most, a moderate distortion in the 6:1 crystal. The HBr frequency in the DME−HBr dimer from the matrix-isolation study[8a] is 2050 cm^{-1}. The higher acid frequency observed in the 6:1 solid strongly suggests that the ether O atom acts as a *double* acceptor in that instance. This follows from the increase in acid frequency for HCl−ether clusters upon addition of the second acid at the double-acceptor position (observed in the DFT calculations and see Figures 4a,c and 5a,b). Moreover, the matrix-isolated $(DME)_2HBr$ bifurcated trimer displayed such a blue shift with respect to the DME-HBr dimer; from 2050 to 2240 cm^{-1}.[8]

A question remains: where, within the 6:1 crystal structure, are the other four HBr molecules located? The remaining acid features, at 2418 and 2465 cm^{-1}, correspond to frequencies close to those of solid HBr (2395 and 2431 cm^{-1}). (Their lower intensity is consistent with DFT calculations, which yield much higher intensity for HX directly connected to O, than for other acid molecules; see Figures 4 and 5 and Table 1.) One possibility is two three-membered chains HBr···HBr···HBr connected to the two lone pairs of the ether O-atom. Figure 5 d displays a

similar configuration for two such (two-membered) chains, connected to DME. The problem with this interpretation is that the acid tail lowers the frequency of the "leading" acid molecules (i.e., the ones connected directly to O) back to the dimer value (compare Figure 5, parts a, b, and d). It is possible that solid-phase packing weakens the bonding of the "tail" molecules to the "leading" ones, thus reducing the frequency shift. It is also possible that the extra four molecules are disconnected from the ones bound to O; in this context, one may note the ease with which the extra acid can be pumped away to form the 4:1 solid (Section 2).

As the acid−ether ratio is reduced from 6:1, the acid bands move smoothly to the red. By the time the composition reaches 1:1, the spectroscopic change is quite dramatic. All HBr absorption is strongly red-shifted, appearing as a very broad (∼500 cm^{-1}) band, badly fragmented by superposed Evan's holes, but centered near 1400 cm^{-1}, i.e., shifted 1160 cm^{-1} from the gas-phase frequency. Again, the source of the Evan's holes, one of which splits the broad band into two parts, is clear from the sharp THF bands of the other crystal phases. Clearly, all HBr molecules are strongly distorted in the 1:1 crystal. The frequency shift is slightly greater than the magnitude (1030 cm^{-1}) reported for strongly distorted HBr molecules on the surface of ice nanocrystals, which are considered on the verge of ionization[3]. The large breadth and the low frequency of the band suggest proton sharing between two heavy atoms.[4]

The simplest physical picture for the 1:1 structure is a solid composed of [THF···H^+···Br^-] units, with the proton shared between the halide and the O atom of the ether. We have one computational example of such asymmetric proton sharing, in a $(H_2O)_7$HCl-cluster structure shown in Figure 3e. This structure was encountered in the course of exploration of possible acid-solvating configurations in acid−water clusters.[3] The corresponding spectrum (Figure 2e) includes a very intense infrared fundamental of the asymmetric proton stretch, similarly to systems in which the proton is shared by two O atoms of the same molecules (of water, methanol, or ether). The asymmetric proton-sharing case corresponds, however, to a higher calculated frequency, in accord with the present interpretation of the experimental data. This is since the HBr−THF 1:1 band is centered near ∼1400 cm^{-1}, while in the dihydrate (H_2O···H^+···OH_2)(Cl^-), the corresponding band is centered at ∼1100 cm^{-1}; see Figure 1A. Other examples of proton sharing between two nonequivalent heavy atoms are known and have been discussed in ref 4 for a variety of systems.

Assuming that the present interpretation is correct, one should note the striking difference between the isolated HBr:THF dimer, which is molecular with slightly perturbed HBr (Figure 4b), and the extended 1:1 solid, in which solvation is sufficient for "halfway" proton transfer. This reflects the effect of mutual solvation of the [THF···H^+···Br^-] units. The difference between parts a and e of Figure 4 can be viewed as an initial step toward such mutual solvation in the solid. Specifically, combining two HX−THF units within a single cluster results in an added ∼200 cm^{-1} frequency redshift. As a related case, one may compare the H_2O−HCl dimer (Table 1), which is molecular, versus the nominally 1:1 H_2O:HCl crystalline monohydrate, in which complete proton transfer occurs (yielding the H_3O^+..Cl^- ionic structure (Figure 1A)). There, the ions mutually solvate each other. Here, the hydrophobic part of THF prevents such full proton transfer, so the limiting case of solid solvation corresponds to proton sharing "only".

The intermediate 4:1 and 2:1 spectra (Figure 7B) represent a transition from the fully molecular 6:1 case to the proton sharing

TABLE 1: Summary of the Calculations for CH_3OH (MeOH), DME, and THF···HX in DFT/B3LYP/Aug-cc-pvDZ[a]

system	*E*(au)	μ(D)	RHCl (A)	ν_{HCl}/I (cm^{-1})/ (kM/mol)
HCl	−460.82771		1.2952	2925/38
HCl···HCl	−921.65777		1.3012	2877/293
			1.2963	2899/46
H_2O···HCl	−537.28117		1.3193	611/893
$(H_2O)_2$···HCl	−613.73857		1.3470	2266/1423
cyclic				
CH_3OH	−115.74239	1.6556		
CH_3OH···HCl	−576.58026	4.030	1.3281	2477/1281.0
CH_3OH···2HCl	−1037.41511	3.102	1.3123	2160/1697.2
			1.3566	2669/621.7
$(CH_3OH)_2$···HCl	−692.33622	3.138	1.3707	2003/2088.1
DME	−155.04602	1.2751		
DME···HCl	−615.88436	3.953	1.3341	2405/1599.4
DME···$2HCl_{biff}$	−1076.71849	4.003	1.3191	2562/1421.0
			1.3191	2617/617.6
DME···$2HCl_{cycle}$	−1076.71789	4.839	1.3588	2122/2270.0
			1.3115	2695/604.4
DME···$4HCl_{biff}$	−1998.38433	1.086	1.3319	2376/2156.8
			1.3086	2467/582.1
			1.3319	2731/88.2
			1.3086	2734/852.3
DME···2HCl···1HCl	−1537.55158	2.678	1.3363	2365/1604/6
			1.3164	2624/781.3
			1.3097	2714/534.6
2DME···2HCl	−1231.77367	0.003	1.3552	2140/0.068
			1.3552	2181/4166.1
THF−*Cs* symmetry	−232.47892	1.6472		
THF···HCl	−693.31894	4.700	1.3474	2239/1954.5
THF...$2HCl_{biff}$	−1154.15437	4.893	1.3262	2462/1710.2
			1.3262	2536/783.2
THF···$2HCl_{cycl}$	−1154.15400	4.951	1.3957	1721/2626.4
			1.3185	2607/805.0
2THF···2HCl	−1386.64264	2.176	1.3643	2050/1143.1
			1.3613	2088/3262.1
HBr	−2574.76318	0.8748	1.4319	2597/10.8
THF···HBr	−2807.25280	4.739	1.4940	1995/2058.9
MP2 HBr	−2573.12466	0.9160	1.4200	2728/9.7
MP2 THF···HBr	−2804.92700	4.0354	1.4826	1976/2009.8

[a] In the bottom 2 lines, MP2 results are shown for THF···HBr (for comparison with DFT results).

1:1 case. In the 4:1 solid, two broad acid bands, with associated structure, fall near 2106 and 2195 cm^{-1}, with narrow THF bands below 2000 cm^{-1}. The situation changes markedly for the 2:1 crystal, as, in addition to a band at 2028 cm^{-1}, a broad band with superposed sharper resonant/anti-resonant features extends from 1900 to 1700 cm^{-1}. The origin of the sharp structure is evident from the 4:1 spectrum, i.e., anti-resonance with the narrow THF overtone bands in the 1700−2000 range. From this view, the HBr stretch modes of the 2:1 crystal produce intense broad bands centered at ∼1785 and 2028 cm^{-1}. In other words, in addition to a "weakly" distorted molecular subset, HBr[1], the 2:1 crystal has HBr[2] molecules with frequencies shifted by ∼800 cm^{-1}, i.e., strongly distorted HBr but not yet in the stage of proton sharing. Incidentally, the magnitude of this shift is similar to that of the 1:2 HBr−DME cluster as deduced from matrix-isolation spectra (820 cm^{-1} [8a]). Such subsets of weakly and more strongly distorted HX molecules will be referred to as HX[1] and HX[2], respectively, throughout this paper.

A possible structural unit for the 4HBr:THF solid may be related to the $(HCl)_4$DME cluster shown in Figure 5d, an ether molecule with two O···HX···HX chains attached to the oxygen lone pairs. The cluster calculation yields however a nearly 300 cm^{-1} frequency splitting between the "leading" and "tail" acid molecules. Even considering that for HBr the frequency range

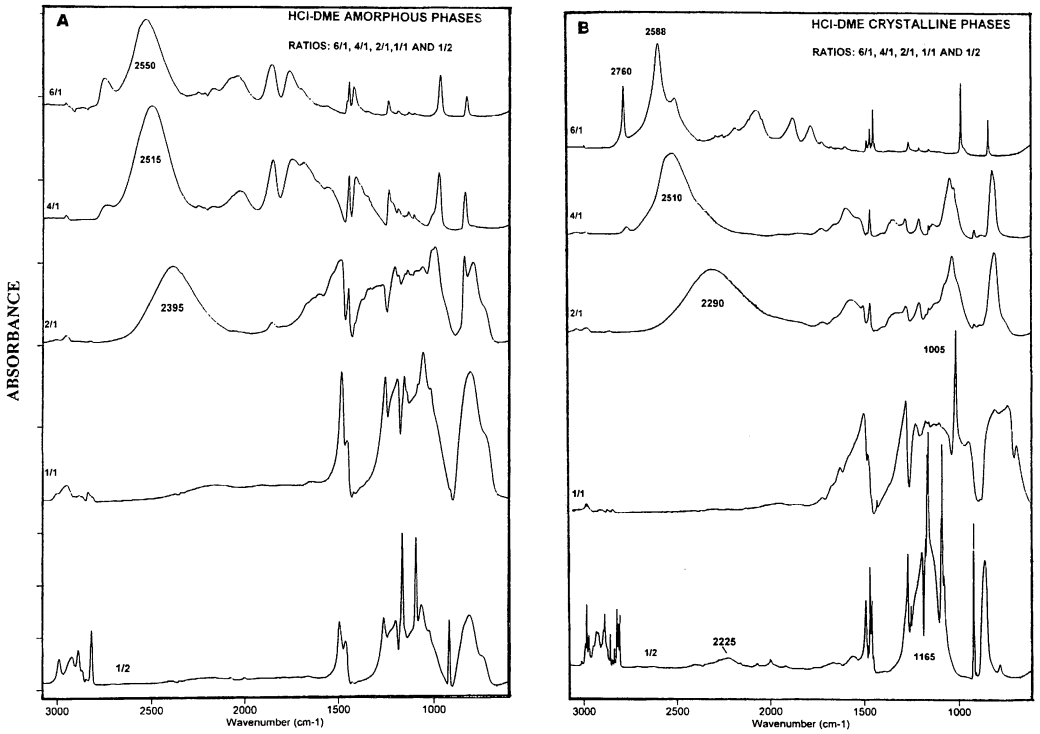

Figure 8. FTIR absorbance spectra of (A) amorphous and (B) crystalline thin films of nHCl:mDME identified by the labels *n*:*m*. Crystalline films, scanned at 80 K, were formed by warming amorphous films prepared at 80 K.

should be reduced with respect to HCl, the observed ~90 cm^{-1} frequency difference appears rather small for this assignment. Most likely, mutual solvation of cluster units is sufficient to red-shift the "tail" acid band.

In contrast, the ~250 cm^{-1} acid-band splitting in the 2HBr:THF spectrum appears too large for a bifurcated structure such as Figure 4c, in which two acid molecules are attached symmetrically to the same ether O atom. An attractive alternative to this strongly asymmetric double-acceptor bonding is a tandem THF···HBr···HBr configuration (Figure 4d) for which the "leading" acid molecule is significantly perturbed, even in the cluster. The "tail" frequency must be then reduced substantially with respect to the isolated cluster, by mutual solvation of the clusters.

A close analogy exists between the band shifts for the four members of the HBr−THF series and the sequential shifts observed by Sobczyk (and described by Zundel[4]) for the crystal system of pentachlorophenol complexed with amines of increasing basicity. That is, the reported effect on a shared proton, of increasing the basicity of an amine acceptor, parallels the effect of increasing THF concentration in the HBr−THF crystal series.

3.3. nHCl:mDME. Amorphous films of five different HCl-DME ratios readily convert to the corresponding crystal phases, i.e., with *n*/*m* ratios 6/1, 4/1, 2/1, 1/1, and 1/2. Spectra of these mostly acid-rich amorphous and crystalline films are presented in Figure 8. There is little difference between the amorphous- and crystalline-phase spectra for 6HCl:DME, HCl:DME, and HCl:2DME, though crystallization is easily recognized by the emergence of numerous sharp (~3 cm^{-1}) bands. Clearly, the local structures of the amorphous and crystalline phases of these three systems are similar, as was noted for each nHBr:THF case in section 3.2; a fact that strongly suggests the presence of similar basic structural elements. By contrast, there is a noticeable change in the overall spectra for 4HCl:DME and 2HCl:DME with crystallization, as intense extremely broad bands near 1750 and 1200 cm^{-1} (Figure 8A) are replaced by distinct but broad bands in the 700−1700 cm^{-1} range. Only a few very weak bands near 1200 cm^{-1} have bandwidths (~4 cm^{-1}) indicative of crystalline phases. Because of these few narrow bands, plus the reproducibility of the spectra of samples prepared by different methods (Section 2), and the sharp change in spectra vs the amorphous phase, the spectra (Figure 8B) are tentatively assigned to *crystalline* 4HCl:DME and 2HCl:DME.

There are both obvious similarities and marked differences between spectra of the crystalline nHCl:mDME series and the nHBr:THF series examined in section 3.2. Similarities include (i) the stepwise red-shift of the molecular H−Cl stretch-mode frequencies as the HX content decreases for the first three members, (ii) the absence of any absorption indicative of weakly distorted HCl in the 1:1 crystal (i.e., above 1800 cm^{-1}), (iii) the dominance of the entire 1:1 spectrum by a broad low-frequency band badly fractured by superposed resonant and anti-resonant states. The notable differences vs nHBr:THF include (i) the emergence of strong broad low-frequency bands already in the 4:1 (and 2:1) phase, (ii) the greater breadth and lower frequency of the dominant band in the 1:1 phase, and (iii) the existence of a 1:2 phase for which the broad low-frequency bands are similar to those of the 4:1 and 2:1 phases, but camouflaged by superposed DME bands from the additional incorporated solvent molecules.

It follows that the main difference, with respect to the HBr case discussed above, can be identified with an enhanced propensity of HCl to form proton-sharing [ether···H^+···Cl^-] units, which can even survive dilution by either acid or ether. (It will be shown below that mHCl:THF displays qualitatively similar behavior to mHCl:DME, so the main source of difference is the acid, not the ether.) We focus first on the crystal spectra. The broad structured band of 1:1 HCl:DME is centered near 1050 cm^{-1}, as compared to ~1400 cm^{-1} for 1:1 HBr:THF, suggesting more effective proton sharing in the former case. For HCl:2DME, one might anticipate even more extensive proton transfer to the solvent, as in (DME···H^+···DME)(Cl^-), i.e., a DME analogue of the HCl dihydrate. However, the spectra do not support this interpretation. Comparison of Figure 8B,

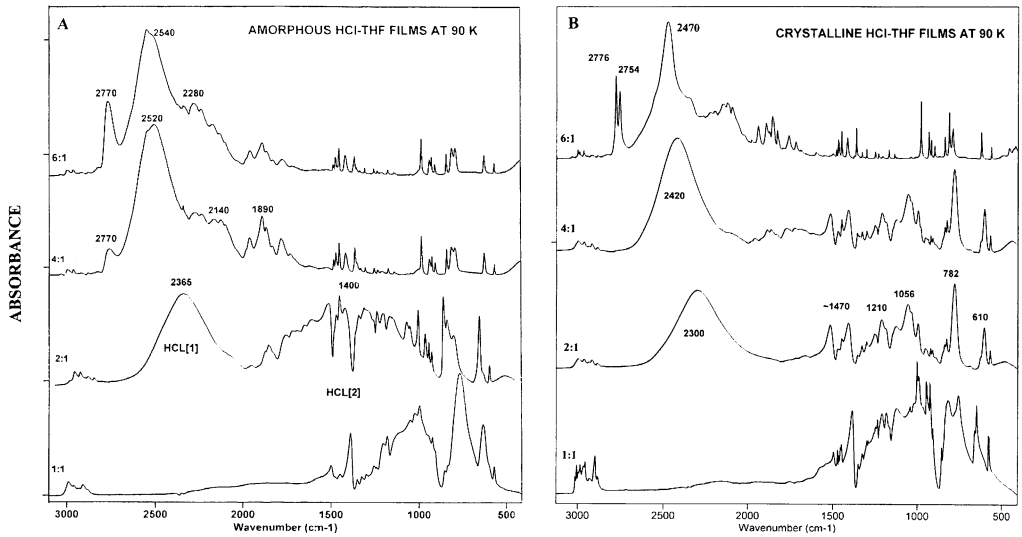

Figure 9. FTIR absorbance spectra of (A) amorphous and (B) crystalline thin films of nHCl:THF identified by the labels *n*:1. Crystalline films, scanned at 80 K, were formed by warming amorphous films prepared at 80 K.

bottom, with Figure 1B, bottom, reveals the presence of bands of weakly perturbed ether molecules. Thus, we prefer an alternative interpretation for HCl:2DME, that of a mixed proton-sharing Zundel unit, [DME..H^+..Cl^-], solvated by the extra DME. The narrowing of the asymmetric-proton-stretch band at ~1100 cm^{-1}, with respect to the 1:1 solid, can then be ascribed to decoupling of proton motions of adjacent units,[4] by the intervening extra ether molecules.

A similar Zundel unit appears to be present in the 2HCl:DME solid; as evidenced by the intense low frequency bands. Here, the extra solvating HCl is likely to be connected to the chloride end of [DME···H^+···Cl^-], although its frequency of 2290 cm^{-1} (Figure 8B) is substantially higher than that assigned to HCl solvating the Cl^- anion in HCl hydrates (2120 cm^{-1} [3]), but a higher frequency is consistent with the incomplete proton transfer in the Zundel unit. The low-frequency band pattern also survives for 4HCl:DME, suggesting that even dilution by 3 acid molecules does not seriously disrupt the Zundel unit. However, the solvating-HCl band moves to the blue with respect to the 2:1 by more than 200 cm^{-1}.

The 6HCl:DME spectrum is quite striking. The broad bands in the 700−1700 cm^{-1} range, assigned to Zundel units in 4:1 and 2:1, are no longer present. Instead, three broad HCl bands (or a single fragmented very broad band?) are present in the 1700~2100 cm^{-1} range, together with bands of more weakly perturbed acid molecules at 2500, 2588, and 2760 cm^{-1}. It is recalled that the 6:1 HBr−THF structure was interpreted above in terms of the ether O atom acting as a double acceptor with respect to two acid molecules, with the remaining acid solvating this cluster. The HCl frequency in the matrix-isolated single/double acceptor cluster with DME is 2310/2480 cm^{-1}. DFT calculations suggest that solvation by additional HCl, of the two acid molecules in the double acceptor configuration, can bring the HCl frequency down but only to near the isolated dimer value; see Figure 5, parts a, b, and d. Thus, the observed 6:1 lower frequency band(s) are unlikely to originate from double-acceptor configurations, despite the high concentration of the acid. Such low frequencies correspond to strongly distorted acid configurations, and (as discussed in the past[3]) single acceptor bonding is required for significant bond stretching (as well as for proton transfer). We therefore suggest that the 1700~2100 cm^{-1} band(s) still originates from an [ether···H^+···Cl^-] unit, with less developed proton sharing (proton closer to the chloride) due to the substantial dilution by the additional HCl. (In these systems, the proton-transfer unit is solvated best by its duplicates.)

Comparison to amorphous-phase spectra reveals a most significant difference for the 4:1 samples. In the 4HCl:DME crystal, the low-frequency pattern indicates a proton-sharing Zundel unit similar to 2:1. However, in the amorphous 4:1 solid, the intense bands are blue shifted above 1500 cm^{-1}, to the same region as for the 6:1. It appears that, at this ratio, symmetry breaking in the amorphous environment is detrimental to proton-sharing. One may note related observations in other systems, e.g., the enhanced presence of molecular acid in amorphous HCl monohydrate, as compared to the crystal[2] and predominantly molecular nitric acid monohydrate in the amorphous phase, versus the fully ionic crystal.[27]

Finally, another curious aspect of the mHCl:nDME spectra is the possible observation of an overtone of the broad 1165 cm^{-1} band of the 1:2 phase at 2225 cm^{-1}. This tentative assignment, which may be especially useful, is based primarily on the observation that, upon warming from 33 to 140 K, the 2225 band blue-shifts ~75 cm^{-1}, as the 1165 cm^{-1} fundamental blue-shifts by ~40 cm^{-1}. If correct, this assignment implies a relatively modest anharmonicity for a proton mode of an analogue of the Zundel cation, reflecting quite a different behavior than has been attributed to the gas-phase Zundel cation.[28]

3.4. nHCl:THF. This acid-ether series is a hybrid of the two considered above: the acid differs from that of the nHBr:THF series of section 3.2 and the solvent is different vs the nHCl:mDME series of section 3.3. There are minor variations, but the spectra of both the amorphous and the crystalline phases of nHCl:THF (Figure 9) parallel those of the HCl−DME series for *n* (*n*/*m*) values of 6, 4, 2, and 1. The changing of the acid of nHX:THF from HBr to HCl has more serious effects that will be emphasized below. The influence of replacing HCl by DCl in the HCl-THF series and HBr by HCl or DCl in the HBr-THF series will also be examined (Section 3.5).

3.4.1. HCl−THF Phases. Consider first the minor effects from replacing the solvent DME with THF (by comparing Figures 8 and 9). The spectra have the same form in regions above 2200 cm^{-1} where the weakly distorted HCl molecules absorb strongly. Further, the amorphous phases of both series reveal broad bands below 2200 cm^{-1} that red-shift rapidly with decreasing *n* value.

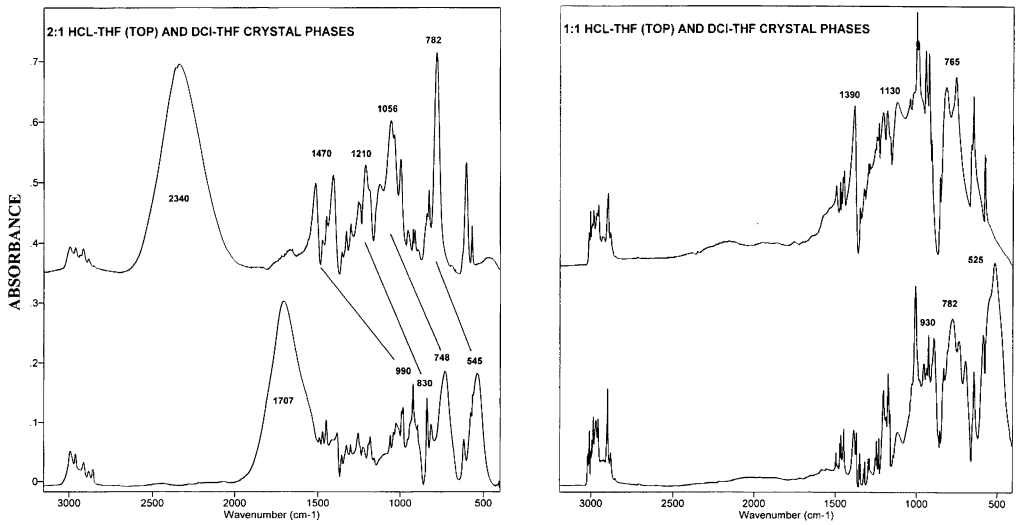

Figure 10. FTIR absorbance spectra of thin crystalline films of left, 2HCl:THF (top) and 2DCl:THF and right, HCl:THF (top) and DCl:THF.

Surprisingly, this shift is somewhat stronger for DME than for the more basic THF. This is most obvious in the $n = 2$ case for which the THF system has a very broad band near 1400 cm^{-1}, whereas DME films have an equally broad band centered near 1200 cm^{-1}. However, the several broad bands in the 700−1700 cm^{-1} range, that emerge for the $n = 4$ and $n = 2$ "crystalline" phases of both the DME and THF systems, not only occupy the same frequency range but display very similar intensity patterns. In particular, the band of greatest *integrated* intensity is near 1100 cm^{-1} for all 4 phases, as well as for HCl:2DME. A stable localized analogue of a Zundel structure, nearly insensitive to surroundings, is implied as noted in section 3.3.

The comparison of the spectra of the crystalline phases of Figure 9B with those of Figure 7B shows the more dramatic effect of replacing HBr with HCl. Though the broad acid-based features for HBr−THF red-shift with decreasing acid content, the shift is gradual and never to frequencies below 1200 cm^{-1}. In contrast, only the 6HCl:THF phase of the HCl−THF series lacks broad bands scattered over the 1700−700 cm^{-1} range. As with the nHCl:mDME series, the 4:1 and 2:1 "crystal" phases contain bands for both weakly stretched HCl and HCl that apparently achieves a proton-sharing structure analogous to the Zundel cation. Also, for the reasons given for the DME series in section 3.3, these intermediate phases are referred to as crystalline although the spectral bandwidths suggest an element of disorder. One may note that partial removal of the acid, from the 2:1 solid, red-shifts the weakly bonded HCl band by ∼140 cm^{-1} and may be indicative of an intermediate structure of some stability, perhaps with a 3:2 ratio.

Interestingly, in the amorphous phase sequence, substantial loss of proton sharing occurs already for 2:1, as opposed to the 4:1 ratio in the case of DME. This finding may be related to the presence of the larger hydrophobic unit of THF, promoting disruption of solvation during symmetry loss.

3.4.2. DCl-THF Phases. Shifts in band positions that accompany deuteration of the acid of the crystalline phases of 2HCl:THF and HCl:THF are shown in Figure 10. Since no observable deuteration of the solvent occurs (e.g., no sharp C−D bands appear in the region of 2000 cm^{-1}), significant spectral shifts can be directly related to modes associated with the solvated acid. From the 1:1 spectra, it is apparent that the very broad absorption centered near 1000 cm^{-1} is red-shifted by 250−300 cm^{-1} upon acid deuteration. This reflects a plausible H−D frequency ratio of 1.3−1.4, similar to that observed for the bands of the Zundel cation of the dihydrate of HCl (see Figure 1A and ref 3).

A better determination of the deuteration shift of individual bands is possible from the 2H(D)Cl:THF spectra of Figure 10 (left panel) in which positions of the distinct bands of the different proton modes are labeled. Though resonant and antiresonant THF−proton states create some uncertainty, the average H/D frequency ratios are estimated to be 1.43 ± 0.03, or the harmonic value within experimental error.

3.5. Variations on the Simple nHX:Ether Substances. Because of the ease with which the acid molecules can diffuse into or from the pure crystalline films described in the above sections, they can be readily interconverted within a single series. Beyond that, it is also possible to switch from one acid to another, so as to grow crystalline films containing two or more different HX species. For example, HCl can be allowed to diffuse into the 1:1 HBr−THF crystal to convert it in sequence to the 2:1, 4:1, and 6:1 crystals with a progressively greater ratio of Cl to Br. Of course, the same sequence can be accessed by using DCl rather than HCl. For this reason, one can examine questions such as (1) in formation of the 2:1 film containing equal amounts of HBr and HCl, do the molecules partition in a preferential manner over the two quite different sites that characterize the 2:1 phase and (2) does isotopic exchange scramble the hydrogen isotopes over the acid molecules within the crystals? The results are quite striking and strongly suggest that the O···HBr bond to the ether is significantly stronger than O···HCl, despite reduced propensity for proton sharing in the former case.

3.5.1 Results for HBr:THF with Added HCl. The spectra of Figure 11A are all from crystal phases generated from the same initial deposit of a 1:1 ratio of HBr and THF. The spectrum (top) of HBr:THF matches the corresponding one of Figure 7B. The other four spectra, reading from top to bottom, are from crystalline complexes formed first by addition (2:1, 4:1, and 6:1) and then removal (4:1) of HCl through the gas phase. This series of spectra is particularly informative. For example, the 2:1 mixed acid spectrum contains a single strong new HCl[1]-stretch band at 2340 cm^{-1}, whereas the HBr[1]-stretch band at 2028 cm^{-1} is weak compared to 2HBr:THF (Figure 7B). These are the HX[1] bands of weakly distorted acid molecules. At the same time, the HBr[2] band near 1790 cm^{-1} retains an integrated intensity greater than the new HCl[1] band while no band can be identified as HCl[2]. This shows with clarity that

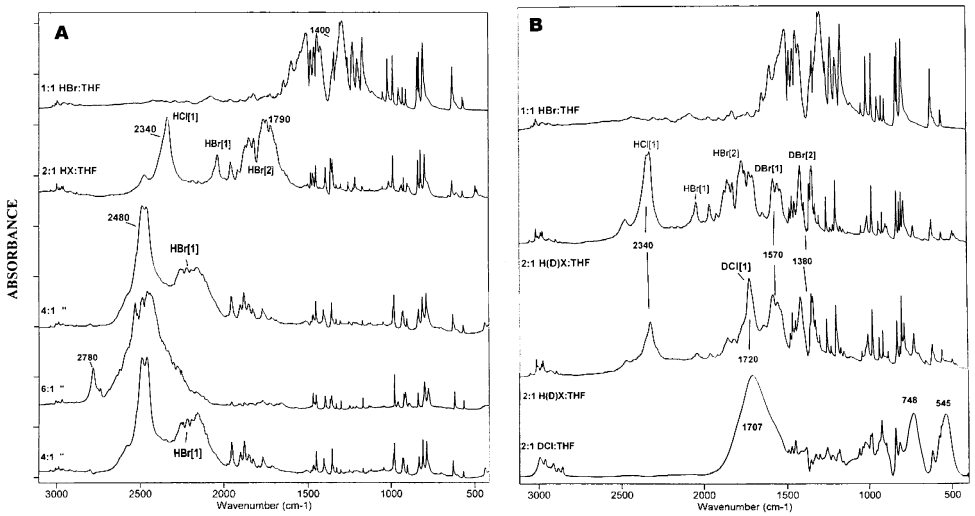

Figure 11. (A) FTIR absorbance spectra of 1:1 crystalline HBr:THF and acid-rich crystalline phases from HCl uptake into the HBr:THF film. The bottom spectrum is after reversal of HCl uptake with conversion back to 4HX:THF from 6HX:THF. (B) FTIR absorbance spectra of 1:1 HBr: THF and 2H(D)X:THF formed by DCl uptake into the 1:1 film (see text for details). The bottom spectrum is that of crystalline pure 2DCl:THF also presented in Figure 6.

the HBr molecules preferentially *retain* the more strongly solvating (distorting) sites while leaving weaker binding sites for the added HCl. Since the computed absolute intensity of the H−X stretch mode increases with HX distortion (Table 1), the ratio of integrated intensities of the HBr[2] and HCl[1] bands, being somewhat greater than unity, is consistent with a phase transition from the 1:1 HBr−THF to the 2:1 phase with incorporation of ∼50% HCl. The 2HBr:THF structure was tentatively interpreted above as one with THF acting as a single acceptor to the HBr[2] molecule, with an additional HBr[1] connected in tandem to HBr[2]. In the mixed HCl:HBr:THF structure, HBr appears to bind to the ether O, and HCl to HBr.

The middle spectrum of Figure 11A is of the 4:1 crystal phase, formed by again doubling the acid content to give an HCl/HBr ratio of 3/1. The HCl[1] band (2480 cm^{-1}) is dominant over the HBr[1] absorption (Figure 7B) centered near 2150 cm^{-1}, as required by the 3/1 ratio. Continued uptake of HCl produced the 6:1 phase of 83% HCl and 17% HBr with the indicated spectrum clearly dominated by a broad HCl[1]-stretch absorption also centered near 2480 cm^{-1}. However, the HCl spectrum, including the single very weakly shifted 2780 cm^{-1} band, differs markedly from the pure 6HCl:THF spectrum of Figure 9B**.** This difference carries over to the many sharp THF bands as well. On the other hand, the THF fingerprint of each of the spectra of Figure 11A matches well the corresponding pattern and precise band positions of the pure HBr−THF crystal spectra of Figure 7B; that is, differences caused by variation of the overall acid−ether ratios are greater than from replacing most of the HBr by HCl within a given phase.

It appears that HBr, present in compositions with acid−ether ratios ranging from 2:1 to 6:1 with a content that varies from 1/2 to 1/6th of the *total HX*, dictates the general nature of the adopted crystal structures, a nature which, like that of the 2:1 to 6:1 crystals of pure HBr with THF (Figure 7), lacks any Zundel component. In no case do the spectra show the intense broad low-frequency bands present in spectra of all except the 6:1 phases of the pure HCl−THF (or HCl−DME) crystals. Finally, the bottom 4:1 spectrum of Figure 11A**,** when compared with the middle spectrum of the same phase, shows the reproducibility of spectra for samples separated by an HCl-load and -pump sequence; and thus, the preferential retention of the HBr. It appears that despite the enhanced tendency for proton sharing, HCl makes a weaker bond to the ether O-atom than does HBr. One possibility is that the 3HCl:HBr:THF and 5HCl:HBr:THF include double acceptor configurations in which the ether O is bonded to one HBr and to one HCl. If double acceptor configurations are in fact present in 4HBr:THF and 6HBr:THF (as suggested in the interpretation of section 3.2), then similarity of spectra suggests presence of double acceptor configurations in the "mixed" cases as well. The acid frequency in the matrix-isolated double-acceptor complex $(HCl)_2$DME is 2480,[8a] similar to the HCl frequency in 3HCl:HBr:THF and 5HCl:HBr:THF.

3.5.2. Results for HBr:THF with Added DCl. The question is whether the preferred O···HBr binding (section 3.5.1) reflects the kenetics rather than the thermodynamics of the system, since the HBr is initially bound to the ether O atom. The following results with HCl replaced by DCl strongly suggest that kinetics is not the reason and that the ether···HBr bond is in fact stronger.

Paralleling Figure 11A, the crystal phases that yielded the two middle spectra of Figure 11B were based on an initial 1:1 crystalline film of HBr:THF (top spectrum), but modified by the uptake of DCl rather than HCl. The spectra of the 2:1 phases can be compared with that of the corresponding phase with ∼equal amounts of chloride and bromide (Figure 11A**)** but lacking any deuterium. Of these two middle spectra of Figure 11B, the top one followed direct DCl uptake into the 1:1 HBr−THF film and, thus, reflects the presence of roughly equivalent molar amounts of bromide, chloride, hydrogen, and deuterium. The lower-middle spectrum is also of the 2:1 crystal but after load-pump cycling of the same sample through the 6:1 crystal phase in which both the D/H and Cl/Br ratios attained levels of ∼5/1.

Isotopic scrambling among acid molecules, presumably through an ionic process, is clearly extensive in the direct uptake of DCl as shown in the top 2:1 spectrum of Figure 11B**.** Isotopic exchange occurred between HBr and DCl. No DCl bands are observed, and the *visible* Cl resides entirely in the weakly bonded HCl[1] band at 2340 cm^{-1}. Both HBr[2] and DBr[2] are intense. DBr[1] and HCl[1] are much more intense than HBr[1]. It is well-known that in hydrogen-bonded systems deuterium adopts preferential positions corresponding to zero-point-energy lowering.[29] However, understanding of the observed pattern would require a detailed vibrational analysis along with absolute intensity data for the various hydrohalide bands.

Flooding of the system with DCl, as in the next spectrum (third from the top), results in extensive, though quite incomplete, replacement of HCl[1] by DCl[1] (at 1720 cm^{-1}) and nearly complete suppression of the HBr[2] band. The THF bands are nearly unaffected, and despite the high exposure to DCl, this spectrum, for a structure dictated by the minority H(D)Br species, is very different from the 2DCl:THF bottom spectrum. The efficient isotopic exchange between DCl and HBr suggests a significant extent of mobility in the system. Thus, the persistence of the DBr[2] band is unlikely to be caused by a kinetic effect from a high barrier to removal. These observations suggest that the DBr-ether bond is stronger than the DCl-ether bond (consistent with the greater acidity of the hydrobromic acid).

Summary

Acid solvation in the liquid phase has been extensively studied in the past, whereas solvation in the crystal phase has received much less attention. However, recently much effort was devoted to acid hydrates, motivated largely by their atmospheric significance.[2,3,30] In contrast to liquid solutions, solid-phase solvation accompanies the formation of distinct crystals of well-defined composition ratios. Mixed acid−solvent crystals offer unique opportunities to generate a range of distinct and potentially well-defined solvating environments and to probe the induced extent of proton transfer.

Here, we have addressed HCl and HBr solvation by methanol and two ethers (DME and THF) in the solid (crystal and amorphous) phase. In the course of the study, several new mixed crystals were discovered: mMeOH:HX, $m = 1-3$; nHX:ether, $n = 1$, 2, 4, and 6; and HCl:2DME was observed as well. The solids display a strikingly broad acid-solvation range, extending from slightly stretched HX molecules, via H-bonding, to full proton sharing with the solvent. Although ultimate determination of the crystal structures must await diffraction studies, considerable insight was gained from the analysis of the spectra in conjunction with DFT calculations on mixed acid-solvent clusters and related protonated-solvent cations.

Acid solvation by methanol was found to parallel that by water. Mixed *ionic* solids analogous to hydrates were observed. Thus, in crystalline MeOH:HX, the cation appears to be the hydronium analogue, $MeOH_2^+$, whereas the cation in mMeOH:HX, $m = 2$ and 3, was identified with the Zundel form $(MeOH)_2H^+$.

Mixed acid−ether crystals display an entirely different physical behavior, attributed to the added hydrophobic groups and lack of proton-donating OH groups to solvate the anions. The result is an apparent absence of acid ionization, beyond proton sharing. In contrast to water and methanol, acid−solvent ratios (much) greater than one were observed. The range of acid states extends from slightly distorted molecular HX, to Zundel-like ether $O\cdots H^+\cdots X^-$ proton-sharing units. The 1:1 acid−ether crystal structures are viewed as a periodic pattern of such units, with proton sharing much enhanced by their mutual solvation. The assignment is based on a lack of molecular acid bands and the presence of broad intense low-frequency bands characteristic of proton-sharing systems.

The Zundel-like units of HCl−ether solids are insensitive to environment, surviving dilution by the ether or the molecular acid. Essentially unshifted intense low-frequency "Zundel" bands are observed for a range of compositions, including HCl:2DME, 2HCl:DME, and 4HCl:DME. In the latter two cases, the excess acid, solvating the Zundel units, was identified by intense bands of "weakly" perturbed molecular HCl. Even in the case of 6HCl:DME, some strongly distorted HCl is present in the system. Similar behavior was observed for nHCl:THF. By contrast, in the case of nHBr:THF, a distinct proton-sharing spectral signature was observed for the 1:1 solid only. Crystals of higher HBr:THF ratios display molecular HBr bands with a range of red shifts. Configurations, in which the ether O atom acts as a double acceptor for acid, appear to be present in the nHBr:THF $n = 4$ and 6 solids. Within the same crystal system the HBr−ether bond seems stronger than the HCl−ether bond, despite the enhanced propensity of the latter for proton-sharing, a conclusion based on spectra of mixed 2:1 HBr/HCl−ether systems. This property may underlie a tendency for HBr to "choose" the crystal structure in mixed HBr−HCl systems.

Much remains to be understood regarding the present results as well as related studies of the hydrates.[2,3] A number of intriguing questions have been raised by these studies of mixed acid−solvent solids. What acid−solvent ratios are preferred by different combinations of constituents and for what reasons? It may not be surprising that similar acid-solvent ratios were obtained for water and methanol, both of which include proton donating and accepting groups. However, why do these ratios never exceed one, whereas for the ether solvents, ratios as great as 6 were observed? At the other limit, why is the acid−water ratio in the crystal hydrates limited by 1/6? Liquid water is an excellent solvent of isolated HCl molecules; but solubility in ice, as low as a part per million,[31] reflects an extreme difference in liquid vs solid solvation. Finally, why do fully ionic ether−acid crystals appear to be nonexistent? For ethers, one could reasonably expect a stable ionic crystal with a Zundel-like cation, $(ether)_2H^+$, and a halide anion. Although the HCl:2DME phase was in fact observed, the spectra indicate a proton-sharing acid−ether unit with a subset of weakly perturbed ether molecules acting as "filler".

Another conceptually interesting issue is the relation between crystal and amorphous acid-solvent phases. At sufficiently low temperatures, amorphous solids of any composition can be prepared. We found, however, that at temperatures at which transient molecular mobility is present during sample deposition, the range of amorphous mixtures that can be prepared is spanned approximately by the range of compositions of the crystalline solids. Excess acid or solvent are excluded from the solid mixture. The question raised also includes the relation between local structures found in the crystals and in the amorphous solids, and the validity of the concept of nucleated amorphous phases.[32] Here, a variety of behaviors was noted. In the case of HBr−THF, the amorphous-phase spectra are a broadened version of those of the crystals of the same acid-ether ratios, strongly suggesting similar local arrangements which vary sharply with composition. The case of amorphous hydrates appears to be quite different. Crystal mono- and hexahydrates include exclusively the hydronium cation, whereas the Zundel form is the basic unit of the di- and trihydrates.[1] On the other hand, all amorphous hydrates, from mono- to hexahydrate, display spectral evidence for coexistence of both cation forms, with varying abundances.[3] In some cases, the loss of symmetry in the amorphous phase results in even more marked structural differences with respect to the crystal. For example, in the ionic acid monohydrates, solvation is enhanced by symmetric mutual arrangement of ionic units (note that $HX-H_2O$ dimers are molecular), whereas loss of order in amorphous HX monohydrates results in a significant increase in the spectral signature of the molecular HX[2,3] (and in the case of nitric acid, the amorphous monohydrate is predominantly molecular[27]). A related result was discussed above for 4HCl:DME, 4HCl:THF,

TABLE 2: B3LYP/Aug-cc-pvDZ Results for Protonated Cluster Ions MH+ and M···H+···M; M = H_2O, CH_3OH, DME, and THF[a]

system	E(au)	R(M···H+···M)	ν/I (cm^{-1})/ (kM/mol)
$H_2O\cdots H^+$	−76.71473		3544/30
			3651/467.5
			3652/468.2
$H_2O\cdots H^+\cdots H_2O$	−153.21587	2.401367	906/2703.7
$CH_3OH\cdots H^+$	−116.03825		3628/192.5
			3714/316.3
$CH_3OH\cdots H^+\cdots CH_3OH$	−231.83294	2.4027	720/2678.1
DME···H+	−155.35689		3693/207.0
DME···H+···DME	−310.45081	2.39624	708/3204.4
THF···H+	−232.80505		3727/212.4
$THF\cdots H^+\cdots THF_{trans}$	−465.33304	2.39917	458/2692.8
$THF\cdots H^+\cdots THF_{cis}$	−465.33303	2.40086	496/2059.5

[a] For MH^+, OH stretch frequencies and intensities are included. For M···H+···M, the most intense vibrational fundamentals are given (related to the asymmetric O···H+···O stretch).

and 2HCl:THF. The crystal spectra include the signatures of the proton-sharing ether O···H+···Cl− units, which, in the amorphous solids, are replaced by bands of strongly perturbed, but molecular, HCl. Loss of symmetry in the amorphous phase commonly results in reduced solvation efficiency.

Appendix. Computational Approach: Calculation of Equilibrium Structures and Vibrational Frequencies of $(HX)_n(Ether)_m$ Clusters

The main difficulty in the interpretation of the HX−solvent crystal spectra is the lack of knowledge of structure of the different materials. Ab initio calculations were therefore carried out on various acid−ether clusters and methanol−acid structures. The objective was to elucidate the extent of acid stretching, and the corresponding frequency shift, as a function of size and configuration. In addition, equilibrium structures and harmonic frequencies were calculated for hydronium-like and Zundel-like protonated ether and methanol ions. The structures of all monomers and complexes were optimized by means of the DFT-B3LYP method, with the augmented correlation consistent basis set aug-cc-pvDZ.[33] This basis set is the largest that could be used for the largest cluster size. This method and the basis set were retained for smaller clusters as well, to obtain trends as a function of size on a consistent level of accuracy. The "tight" or "very tight" options were used in all geometry optimizations. Energies were converged to ∼0.01 mirco-Hartree, and the corresponding root-mean-square deviations of energy gradient with respect to nuclear coordinates were about 10 micro-Hartree/Bohr.

The resulting energetics, HX bond lengths, dipole moments, harmonic frequencies, and band intensities, for molecular structures of MeOH, DME, and THF interacting with the acid, are reported in Table 1. The results for water−acid clusters, which are shown for comparison, were adopted from ref 3. The acid−water and acid−methanol dimers are O-bonded. The trimers are cyclic. Most of the acid-ether clusters are displayed in Figures 4 and 5. Note the typically very high intensity of the HX-stretch mode for O-bonded HCl molecules in all of the clusters.

Table 2 shows the ab initio results for protonated cluster ions of water, methanol, and ether. The structures of the Zundel-type ions are shown in Figure 3, and the corresponding harmonic spectra are shown in Figure 2. Each spectrum includes very intense bands corresponding to the O···H+···O asymmetric stretch. In the case of THF, this motion contributes to three intense fundamentals. We also have one example of asymmetric proton sharing between Cl and O, which is relevant to the present study. Specifically, in a previous investigation of mixed water clusters with HCl, an $(H_2O)_7\cdots HCl$ structure was obtained in which R(H···Cl) = 1.43 Å and R(H···O) = 1.38 Å (MP2-level calculation in aug-cc-pvDZ basis; structure (k) of ref 3, here displayed in Figure 3e). It is seen that a very intense asymmetric stretch band is also present in the case of proton sharing between O and Cl. The exact frequency values for the different Zundel-type ions should not be taken too seriously, since anharmonic corrections are expected to be large.[6] However, the qualitative result that a very intense band below 1500 cm^{-1} indicates proton sharing between two heavy atoms is likely to be correct.

Acknowledgment. Support of this research by the National Science Foundation and the Binational Science Foundation is gratefully acknowledged.

References and Notes

(1) Monohydrate: Yoon, Y. K.; Carpenter, G. B. *Acta Cryst*. **1959**, *12*, 17. (b) Dihydrate: Lundgren, J. O.; Olovsson, I. *Acta Cryst.* **1967**, *23*, 966. (c) Trihydrate: Lundgren, J. O.; Olovsson, I. *Acta Cryst*. **1967**, *23*, 971. (d) Hexahydrate: Taesler, I.; Lundgren, J. O. *Acta Cryst*. **1978**, *B34*, 2424.

(2) Delzeit, L.; Rowland, B.; Devlin, J. P. *J. Phys. Chem.* **1993**, *97*, 10312.

(3) Buch, V.; Sadlej, J.; Uras-Aytemiz, N.; Devlin, J. P. *J. Phys. Chem. A* **2002**, *41*, 9374.

(4) Zundel, G. *Proton Polarizability of Hydrogen Bonds and Proton-Transfer Processes; Their Role in Electrochemistry and Biology*; Institut fur Physikalische Chemie der Universitat Muchen: Muchen, 1997: Chapter 7, p 169; *Adv. Chem. Phys.* **2000**, *111*, 1.

(5) Agmon, N. *Chem. Phys. Lett.* **1995**, *244*, 456. Ando, K.; Hynes, J. T. *J. Phys. Chem. B* **1997**, *101*, 10464. Tuckerman, M.; Laasonen, K.; Sprik, M.; Parrinello, M. *J. Chem. Phys.* **1995**, *103*, 150. Vuillemier, R.; Borgis, D. *J. Phys. Chem. B* **1998**, *102*, 4261; *J. Mol. Struct.* **2000**, *117*, 552.

(6) Vener, M. V.; Kuhn, O.; Sauer, J. *J. Chem. Phys.* **2001**, *114*, 240.

(7) Bienko, A. J.; Latajka, Z.; Sawka-Dibrowolska, W.; Sobczyk, L.; Ozeryanskii, V. A.; Pozharskii, A. F.; Grech, E.; Nowicka-Scheibe, J. *J. Chem. Phys.* **2003**, *119*, 4313.

(8) (a) Barnes, A. J.; Wright, M. P. *J. Mol. Struct.* **1986**, *135*, 21. (b) Ault, B. S.; Steinback, E.; Pimentel, G. C. *J. Phys. Chem.* **1975**, *79*, 615.

(9) Schriver, L.; Loutellier, A.; Burneau, A. *Chem. Phys. Lett.* **1979**, *60*, 471. Schriver, L.; Loutelier, A.; Burneau, A.; Perchard, J. P. *J. Mol. Struct.* **1982**, *95*, 37.

(10) Millen, D. J.; Schrems, O. *Chem. Phys. Lett.* **1983**, *101*, 320. Asselin, P.; Dupuis, B.; Perchard, J. P.; Soulard, P. *Chem. Phys. Lett.* **1997**, *268*, 265. Asselin, P. Soulard, P.; Alikhani, M. E.; Perchard, J. P. *Chem. Phys.* **1999**, *249*, 73.

(11) See, for example: Wojcik, M. J. *Int. J. Quantum Chem.* **1986**, *29*, 855.

(12) Seel, R. M.; Sheppard, N. *Spectrochim. Acta* **1969**, *25A*, 1287. Lassegues, J. C.; Cornut, J. C.; Huong, P. V.; Grenie, Y. *Spectrochim. Acta* **1971**, *27A*, 73.

(13) Loutelleir, A.; Schriver, L.; Burneau, A.; Perchard, J. P. *J. Mol. Struct.* **1982**, *82*, 165.

(14) Nowak, M. J.; Szczepaniak, K.; Baran, J. W. *J. Mol. Struct.* **1978**, *47*, 307.

(15) Park, S.-C.; Maeng, K.-W.; Kang, H. *Chem. Eur. J.* **2003**, *9*, No.8, 1706.

(16) Marechal, Y.; Witkowski, A. J. *Chem. Phys.* **1968**, *48*, 3697.

(17) Devlin, J. P.; Uras, N.; Sadlej, J.; Buch, V. *Nature* **2002**, *487*, 269.

(18) Svanberg, M.; Pettersson, J. B. C.; Bolton, K. J. *J. Phys. Chem. A* **2000**, *104*, 5787.

(19) Re, S.; Osamura, Y.; Suzuki, Y.; Schaefer, H. F., III *J. Chem. Phys.***1998**, *109*, 978.

(20) Conley, C.; Tao, F. M. *Chem. Phys. Lett.* **1999**, *301*, 29.

(21) Pedone, D.; Armand, M.; Deroo, D. *Solid State Ionics* **1988**, *28−30*, 1729.

(22) Uras-Aytemiz, N.; Joyce, C.; Devlin, J. P. *J. Phys. Chem. A* **2001**, *105*, 10497.

(23) Wang, X.; Schultz, A. J.; Halpern, Y. *J. Phys. Chem. A* **2002**, *106*, 7304.

(24) Evans, J. C. *Spectrochim. Acta* **1962**, *18*, 507.

(25) Scherer, J. R. In *Advances in Infrared and Raman Spectroscopy*, Clark, R. J. H., Hester, R. E., Eds.; Heyden & Son Ltd.: London, 1978; Vol. 5, Chapter 3.
(26) Nakamoto, K. *Infrared Spectra of Inorganic and Coordination Compounds*; Wiley: New York, 1963.
(27) Ritzhaupt, G.; Devlin, J. P. *J. Phys. Chem.* **1991**, *95*, 90.
(28) Asmis, K. R.; Pivonka, N. L.; Santambrogio, G.; Brummer, M.; Kaposta, C.; Neumark, D. M.; Woste, L. *Science* **2003**, *299*, 1375.
(29) See, for example, Engdahl, A.; Nelander, B. *J. Chem. Phys.* **1987**, *86*, 1819; Coudert, L. H.; Lovas, R. J.; Suenram, R. D.; Hougen, J. T. *J. Chem. Phys.* **1987**, *87*, 6290. Devlin, J. P. *J. Chem. Phys.* **2000**, *112*, 5527.
(30) Xueref, I.; Domine, F. *Atmos. Chem. Phys. Discuss.* **2003**, *3*, 4037.
(31) Thibert, E.; Domine, F. *J. Phys. Chem. B* **1997**, *101*, 3554.
(32) Uras-Aytemiz, N.; Joyce, C.; Devlin, J. P. *J. Phys. Chem. A* **2001**, *105*, 10497.
(33) Dunning T. H. *J. Chem. Phys.* **1989**, *90*, 10.